Blocking Cx43 alleviates neuropathic pain mediated by P2X4 receptor in CCI rats

Juping Xing
Nanchang University
Hongji Wang
Nanchang University
Lisha Chen
Nanchang University
Hanxi Wang
Nanchang University
Huan Huang
Nanchang University
Jiabao Huang
Nanchang University
Changshui Xu (changshui-xu@163.com)
Nanchang University https://orcid.org/0000-0002-5192-6167

Research article

Keywords: Neuropathic pain, Connexin43, Purinergic 2X4, Dorsal root ganglion

Posted Date: April 18th, 2022

DOI: https://doi.org/10.21203/rs.3.rs-1512422/v1

Abstract

Background: The current treatment strategy for pain is still the application of traditional analgesic drugs to relieve pain but with many side effects. Therefore, neuropathic pain is a growing concern in the medical community, and the search for new analgesic targets for neuropathic pain has become a new hot spot. In this study, we examined whether Cx43 have the key role in response to peripheral nerve injury in P2X4 receptor-mediated neuropathic pain rats, thereby activating large numbers of satellite glial cells and neurons.

Methods: A rat model of chronic compression injury of the sciatic nerve was established, and the dorsal root ganglion and serum were examined at the relevant molecular levels using western blot, quantitative fluorescent PCR, multiplex immunofluorescence and ELISA.

Results: Our results confirm an important role for Cx43 in P2X4 receptor-mediated neuropathic pain. The release of ATP from Cx43 into the extracellular space activates itself and neighboring satellite glial cells and triggers a cascade amplification effect of inflammation, creating an inflammatory microenvironment that ultimately leads to neuronal sensitization of neuropathic pain in CCI rats.

Conclusions: In brief, blockade of CX43 could attenuate P2X4 receptor-mediated neuropathic pain in rats suffering from CCI, and Cx43may be promising therapeutic targets for the development of novel pharmacological agents in the management of neuropathic pain.

1. Introduction

Neuropathic pain refers to allodynia and hyperalgesia caused by diseases of the central or peripheral nervous system(1, 2), and it can cause chronic neuropathic pain through many pathways in the case of peripheral nerve injury(3). This perception that produces a pain response is the result of neural pathway activity. This neural pathway activity is believed to be caused by the activation of receptors and ion channels and subsequent ectopic firing of neurons(4). The neurons responsible for spreading nerve pain are called "nociceptors", and nociceptor cell bodies are located in the dorsal root ganglia(5).It has been well documented that the release of inflammatory factors and chemokines such as ATP, CXCL-1, IL-1β and TNF-α by glial cells plays an important role in the establishment and maintenance of neuropathic pain(6-9). In addition, inflammatory factors released by primary afferent neurons further activate glial cells(10). Glial cells respond rapidly to peripheral nerve injury and are activated by altered expression of a variety of genes, most commonly the purinergic 2X4 (P2X4) receptor, an ATP-gated cation channel(11).

P2X4 receptors trigger neuroinflammation in response to high extracellular ATP concentrations(11, 12). Nerve inflammation can develop into chronic pain if left untreated(13). ATP has been considered an intracellular energy source in the past, but now ATP has an important role as an extracellular signaling molecule between neurons and glial cells(14). In neuropathic pain, the substantial accumulation of extracellular ATP triggers a cascade of amplified inflammatory responses(15, 16). Connexin43 (Cx43) is involved in maintaining inflammatory signaling by promoting the release of ATP(17). Six connexins form

hemichannels, two hemichannels dock with each other to form gap junctions, and a hemichannel is a connexin hexamer(18, 19). Gap junctions are the main mechanism of the exchange of metabolites and electrical signals between cells. These connections are essential in coordinating cell signal transduction, such as the propagation of electrical signals and the transmission of signals from second messengers(20).

In this study, we examined the expression of Cx43, P2X4, as well as the levels of the cytokines ATP, TNF-α and IL-1β, in the DRG of CCI rats. We used Gap26 to blockCx43, detected changes in the expression of P2X4 and examined the phosphorylation levels of p38, ERK and NF-kB proteins. Our data suggest that ATP released via Cx43 has an important role in the activation of satellite glial cells, the cascade amplification effect of inflammation, the formation of the inflammatory microenvironment and neuronal sensitization. The p38, ERK, and NF-kB signaling pathways have been shown to be involved in the development of neuropathic pain processes. Thus, ATP released via Cx43 have a crucial role in the rat model of chronic constriction injury (CCI)of the sciatic nerve.

2. Materials And Methods

2.1 Animal model and groups

Sprague–Dawley rats (180–220 g) were purchased from Changsha Tianqin Biotechnology Co., Ltd. (Changsha, China). Laboratory animals were provided free access to water and food in a room with a controlled temperature and luminosity (22 ± 2 °C, 50% humidity, and 12-h light/dark cycle). We attempted to reduce the pain of experimental animals and reduce the number of animals during the experiment. All experiments were reviewed and approved by the Animal Management Committee of Nanchang University. Neuropathic pain is produced by inducing chronic constriction injury of the sciatic nerve in rats. Briefly, rats were anaesthetized with urethane combined with xylazine. First, the sciatic nerve in the left thigh was isolated, and then four ligatures were ligated around the sciatic nerve. The distance between each ligature was one millimeter. The ligatures were loosely ligated until slight movement of the ipsilateral hind limb was observed. Finally, the surgical site of the rat was disinfected with iodophor. The operation used for the rats in the sham group was the same as that for the rats in the CCI group, but the sciatic nerve was not ligated. Successful establishment of the model is defined by spontaneous foot elevation, toes curled together, sloping rows and a reduction in mechanical and thermal pain sensitivity of at least 30%.

2.2 Drugs and administration

The Cx43 mimetic (Gap26), which was purchased from GIPBIO, was mixed with saline prior to use. The drug was administered to the animal by intrathecal injection through spinal puncture between the L5 and L6 levels to deliver 10 μl (20 μg) of drug into the cerebrospinal fluid. The drug was injected on Days 7, 9, 11 and 13 after the procedure.

2.3 Behavioral Analysis

Measurement of the mechanical withdrawal threshold (MWT): The rats were placed in a clear plastic box (22×12×22 cm) on top of a stainless-steel wire mesh. The temperature in the room was maintained at 25 °C at all times, and the rats were allowed a few minutes to acclimate. The left hindfoot was randomly stimulated using an electronic analgesia apparatus (BME-404, Tianjin, China) at a pressure of 0–50 g in rats by investigators with no prior knowledge of the groups. The rats were stimulated 10 times at 10 second intervals. The mean value of each group of rats was recorded as their MWT.

Measurement of the thermal withdrawal latency (TWL): The rats were placed in a clear bottomless square acrylic box (22×12×22 cm) on a glass plate. The left hindfoot of the rat was irradiated with a heat beam using a fully automatic plantar analgesia apparatus (BME-410C, Tianjin, China). The heat beam was turned off when the rat withdrew its left hindfoot. The time between heat beam onset and heat beam off (withdrawal of the rat's hind foot) was recorded as the TWL. The left hind foot of rats was randomly alternately stimulated at 5-minute intervals by investigators with no prior knowledge of the groups. Each rat was measured 6 times. The maximum duration of the heat beam exposure was 30 seconds.

2.4 Quantitative real-time reverse transcription-polymerase chain reaction (qPCR)

L4–6 DRGs were isolated from rats on Day 13 after surgery, and the isolated ganglia were immediately washed with 0.01 M PBS, dispensed in RNA stabilization solution (Thermo Fisher Scientific, USA) and stored at -80 °C. Total RNA was extracted from DRGs using the TransZol UP Plus RNA Kit (TransGen Biotech, Beijing, China). One milliliter of TransZol Up was added to 50–1100 mg of sample and homogenized using a nuclease-free glass homogenizer. After an incubation for 5 min, a portion of chloroform was added, shaken vigorously for 30 seconds and incubated for 3 min at room temperature. The mixture was centrifuged at 10,000 g for 15 min at 4 °C. The colorless aqueous phase was transferred to a new EP tube, an equal volume of anhydrous ethanol was added and the sample was mixed by inversion. The resulting solution was added to a centrifuge column and centrifuged at 12,000 g for 30 seconds, discarding the effluent. Five hundred microliters of CB9 were added, the sample was centrifuged twice at 12,000 g for 30 seconds each time and the effluent was discarded. Then, 500 µl of WB9 were added and centrifuged twice at 12,000 g for 30 seconds each, discarding the effluent. The sample was centrifuged at 12,000 g for 2 min at room temperature to completely remove any residual ethanol. The centrifuge column was placed in an RNase-free tube, and 50–200 µl of RNase-free water were added and incubated with the column for 1 min at room temperature. The sample was centrifuged at 12,000 g for 1 min at room temperature to elute the RNA. The RNA was stored at -80 °C. The RNA was then reverse transcribed to complementary DNA (cDNA) templates using EasyScript One-step gDNA Removal and cDNA Synthesis SuperMix (TransGen Biotech, Beijing, China) by incubating the sample at 42 °C for 15 minutes. The cDNA templates were further amplified with qPCR using PerfectStart Green qPCR SuperMix (TransGen Biotech, Beijing, China). P2X4 and Cx43 mRNA expression levels were quantified using a Bio–

Rad fluorescent quantitative PCR instrument (CFX Connect). The qPCR cycling conditions were set according to the manufacturer's reaction parameters: predenaturation at 94 °C for 30 seconds, 44 cycles of three steps: 94 °C for 5 seconds followed by 55 °C for 15 seconds and 72 °C for 10 seconds for amplification (total Volume 20 μl). ΔCT was calculated as the average threshold cycle (CT) value of Cx43 mRNA or P2X4 mRNA minus the average CT value of GAPDH (ΔCT = CT target – CT reference). ΔΔCT = ΔCT test sample – ΔCT calibrator sample. Finally, we determined the relative quantity (RQ) of Cx43 or P2X4 expression according to the acknowledged equation: $RQ=2^{-\Delta\Delta CQ}$. The forward primer sequence of P2X4 was 5'-CCATCTGCATAGTGACGGCT-3'. The reverse primer sequence was 5'-TGTGCACTCTTCCCACTGTC-3'. The forward and reverse primer sequences of GAPDH were 5'-GCATCTTCTTGTGCAGTGCC-3' and 5'-TACGGCCAAATCCGTTCACA-3'.

2.5 Western blot

The isolated L4–6 DRGs were stored in a freezer at -80 °C. Tissue samples were homogenized by mechanical disruption in RIPA lysis buffer containing protease inhibitors and protein phosphatase inhibitors using a glass homogenizer. After the tissue was completely lysed, the liquid was transferred to a new EP tube and centrifuged at 4 °C and 14,000 g for ten minutes, and the supernatant was collected as the protein extract. Protein loading buffer was added to the protein extract in proportion, boiled in boiling water for 5 min, allowed to cool and stored in aliquots at -20 °C. Protein concentrations were measured using the BCA protein assay (Applygen, Beijing, China). Each lane was spiked with thirty micrograms of protein and electrophoretically separated on SDS–PAGE gels (8%-15%). After electrophoresis, the proteins were transferred to polyvinylidene fluoride (PVDF) membranes. Afterwards, the PVDF membrane was incubated for 2 hours at room temperature with a blocking buffer containing 5% skim milk powder or 5% bovine serum albumin. Next, the blots were incubated with an antibody against P2X4 (1:1000, rabbit, Alomone), Cx43 (1:1000, goat, SICGEN), CXCR2 (1:200, rabbit, abcam), P38 (1:1000, rabbit, Cell Signaling), phosphor-P38 (1:500, rabbit, Cell Signaling), ERK1/2 (1:1000, rabbit, Cell Signaling), phospho-ERK1/2 (1:1000, rabbit, Cell Signaling), JNK (1:1000, rabbit, Cell Signaling), phospho-JNK (1:500, rabbit, Cell Signaling), P65 (1:500, rabbit, Cell Signaling), or phospho-P65 (1:500, rabbit, Cell Signaling) , IL-1β(1:200, rabbit, Affinity) and TNF-α(1:400, rabbit, Boster) at 4 °C overnight. The blots were probed with an antibody against GAPDH (1:1000, Mouse, BOSTER) to ensure consistent protein loading. The next day, these blots were further incubated with horseradish peroxidase-conjugated secondary antibodies (1:2000, BOSTER) and then exposed to ChemiDoc^{TM}XRS+ (Bio–Rad). Finally, the intensity of the protein bands was determined using NIH ImageJ software.

2.6 Immunohistochemistry and immunocytochemistry

The isolated L4–6 DRGs were immediately treated with 0.01 M PBS on Day 13 after surgery, and then the DRGs were fixed with 4% paraformaldehyde (PFA) for 2 hours. After fixation, the tissues were washed 3 times with 0.01 M PBS and then dehydrated overnight at 4 °C in 10%, 20% and 30% sucrose solutions.

Finally, the tissue was infiltrated with an OCT mixture (optimum cutting temperature compound) and sectioned with a cryostat for final immunohistochemical treatment. For multiplex immunofluorescence staining, we chose primary antibodies raised in different species and secondary antibodies against the same species to avoid interference with immunofluorescence. Tissue sections were first washed 3 times with 0.01 M PBS, permeabilized with 0.3% Triton-X for 15 minutes, and then washed 3 times with 0.01 M PBS. Next, the sections were incubated with 10% donkey serum at 37 °C for 1 hour. Afterwards, the sections were incubated overnight at 4 °C with the following primary antibody mixture: P2X4(1:100, rabbit, Alomone), Cx43(1:100, goat, Sigma), and GFAP (1:100, mouse, Biolegend). The next day, the sections were washed 3 times with 0.01 Sections were incubated for 1 hour at room temperature with the following mixture of secondary antibodies: TRITC-conjugated donkey anti-rabbit (1:200, donkey, Jackson ImmunoResearch), FITC-conjugated donkey anti-goat (1:200, donkey, Jackson ImmunoResearch), and allophycocyanin-conjugated donkey anti-mouse (1:200, donkey, Jackson ImmunoResearch). The images were finally captured using an Olympus laser scanning confocal microscope (FV3000).

2.7 Enzyme-linked immunosorbent assay (ELISA)

ELISA kits for ATP and CXCL1 were purchased from CAMILO. On Day 13 after surgery, we obtained blood samples from the carotid artery of rats and centrifuged them to obtain serum. Rat serum was stored at -80 °C prior to use. ELISAs were performed using a microplate reader (PerkinElmer, USA) according to the ELISA reagent manufacturer's instructions. A standard curve was included with each experiment.

2.8 Molecular Docking

The Cx43.pdb file were downloaded from http://www.rcsb.org/pdb/home/home.do, and the gap26. sdf file was downloaded fromhttps://pubchem.ncbi.nlm.nih.gov/.Autodock Tools soft was used for molecular docking.

2.9 Statistical method

GraphPad Prism v8.4.0 software was used for graphing and data analysis. The experimental results were expressed as mean ± standard error (mean ± SEM). Comparisons among multiple groups were performed using one-way analysis of variance (ANOVA) combined with least significant difference (LSD). P values less than 0.05 were considered statistically significant.

3. Results

3.1 Blocking Cx43 reduced the sensitivity of rats with CCI to mechanical and thermal pain

In 1988, Professors Bennett and XieYikuan et al. reported criteria for establishing the CCI model and the behavioral manifestations of pain, with nociceptive hypersensitivity to injurious thermal and mechanical stimuli at 2 days after surgery(21). We performed behavioral tests on rats at different time points postoperatively (Days -1, 0, 1, 3, 5, 7, 9, 11 and 13). Mechanical pain sensitivity and thermal pain sensitivity were in the normal range in all groups of rats prior to surgery. Pain sensitivity was increased in rats with ligated sciatic nerves starting on postoperative Day 3. However, behavioral manifestations recorded 2 hours after an intrathecal injection of Gap26 showed that Gap26 consistently reversed pain symptoms in rats (Figure 1). Based on these data, Cx43 is involved in the neuropathic pain behavior of rats with chronic compression injury to the sciatic nerve.

3.2 Blocking Cx43 reduces the expression levels of Cx43 and P2X4 receptors in the DRG of CCI rats

In the present study, we examined the expression of Cx43 and P2X4 receptors in the DRG of each group of experimental rats using western blot analysis. One-way ANOVA results showed a significant increase in Cx43 expression in the DRG of CCI rats compared to the sham group ($P<0.0001$). Cx43 expression levels were significantly lower in the Gap26 group than in the CCI group ($P<0.0001$) and the Vehicle group ($P<0.0001$). Cx43 expression was not statistically significantly different between the CCI and Vehicle groups ($P>0.05$) (Figure 2A). Significantly increased expression of P2X4 receptors was observed in the DRG of CCI rats compared to the sham group ($P<0.01$). Significantly lower expression of the P2X4 receptor was detected in the Gap26 group than in the CCI group ($P<0.01$) and the Vehicle group ($P<0.01$). P2X4 receptor expression was not statistically significant between the CCI and Vehicle groups ($P>0.05$) (Figure 2B). Multiplex immunofluorescence staining of DRG sections from CCI rats showed colocalization of Cx43, P2X4 receptors and GFAP (Figure 2C). These data suggest that Gap26 reverses the increased expression of Cx43 and P2X4 receptor proteins in the CCI rat model group.

3.3 Effect of Gap26 on levels of the P2X4 mRNAs in the DRGs of CCI rats

P2X4 mRNA levels in the rat DRG were detected using real-time fluorescence quantitative PCR (Figure 3). One-way ANOVA results showed significantly increased expression of the P2X4 mRNA in DRG of CCI rats compared to Sham rats ($P<0.001$). Significantly lower P2X4 mRNA levels were detected in the DRG of rats from the Gap26 group compared to CCI rats ($P<0.001$). The difference between the CCI and Vehicle groups was not statistically significant ($P>0.05$). Based on these results, Cx43 mRNA transcription is not affected by Gap26, but Gap26 affects the transcription of the P2X4 mRNA and influences the expression of P2X4 receptor proteins.

3.4 Effect of blocking Cx43 on activation of p38 and ERK signaling pathways

We used western blot to detect the role of the p38 and ERK signaling pathways in CCI rats and to examine the effect of Gap26 on the p38 and ERK signaling pathways (phosphorylated extracellular signal-regulated kinase P-p38 and P-ERK) in the DRGs of CCI rats. The level of P-p38 was significantly increased in the DRG of CCI rats compared to the sham group ($P<0.0001$). The level of P-p38 was significantly lower in the Gap26 group than the CCI group ($P<0.0001$) and the Vehicle group ($P<0.001$). The level of P-p38 was not statistically significantly different between the CCI and Vehicle groups ($P>0.05$) (Figure 4). P-ERK levels were significantly increased in the DRG of CCI rats compared to the sham group ($P<0.01$). P-ERK levels were significantly lower in the Gap26 group than in the CCI group ($P<0.01$) and the Vehicle group ($P<0.01$). P-ERK levels were not statistically significantly different between the CCI and Vehicle groups ($P>0.05$) (Figure 4). Thus, ligation of the sciatic nerve leads to the phosphorylation and activation of p38 and ERK in CCI rats. Gap26-mediated reversal of nociceptive hyperalgesia in CCI rats is associated with reduced phosphorylation and activation of p38 and ERK.

3.5 Effect of blocking Cx43 on activation of NF-κB signaling pathways

To determine the underlying molecular mechanisms of neuronal sensitization, we also monitored the activation of the transcription factor nuclear factor-kB (NF-kB).NF-kBis an important intracellular nuclear transcription factor. It is involved in the inflammatory response in the body. We performed western blot and immunofluorescence assays to examine the role of the NF-κB signaling pathway in the DRG of CCI rats. The effect of Gap26 on the NF-κB signaling pathway (phosphorylated extracellular signal-regulated kinase P-p65) in the DRGs of CCI model rats was also examined. The level of P-p65 was significantly increased in the DRG of CCI rats compared to the sham group ($P<0.0001$). A significantly lower level of P-p65 was detected in the Gap26 group than in the CCI group ($P<0.0001$) and the Vehicle group ($P<0.0001$). The level of P-p65 was not significantly different between the CCI and Vehicle groups ($P>0.05$) (Figure 5). Immunofluorescence colocalization of p65 with DAPI was detected using laser scanning confocal microscopy to reveal whether p65 enters the nucleus. The distribution of p65 in the nuclei of CCI rats was significantly higher than that of the sham group. The distribution of p65 in the nucleus was significantly reduced in the Gap26 group compared to the CCI group. Based on these results, sciatic nerve injury leads to increased phosphorylation of NF-κB in CCI rats. Reduced nociceptive sensitization in CCI rats induced by Gap26 is associated with the reduced phosphorylation and activation of NF-κB.

3.6 The content level of TNF-α, IL-1β ATP.

Peripheral nerve injury induces increased release of inflammatory factors and chemokines. The release of inflammatory factors further activates DRG satellite glial cells, which in turn release more cytokines,

causing a cascade amplification of inflammation and ultimately leading to abnormal neuronal excitation. We therefore examined the expression of TNF-α and IL-1β in the DRG of each group of rats using western blot assays. One-way ANOVA showed significantly increased expression of TNF-α and IL-1β in the DRG of CCI rats compared to the sham group ($P<0.01$). TNF-α and IL-1β expression levels were significantly lower in the DRG of Gap26 rats compared to the CCI group ($P<0.01$) and the Vehicle group ($P<0.01$). The expression of TNF-α and IL-1β was not statistically significantly different between the CCI and Vehicle groups ($P>0.05$) (Figure 7). We measured the levels of ATP in the serum of each group of rats using ELISAs. The results showed a significant increase in the serum levels of ATP in CCI rats compared to the sham group ($P<0.001$). Significantly lower levels of ATP were detected in serum from Gap26-treated rats compared to the CCI group ($P<0.01$) and Vehicle group ($P<0.01$). No significant differences in the levels of ATP were observed between the CCI and Vehicle groups ($P>0.05$) (Figure 6).

3.7 Molecular docking

The results of molecular docking showed that the binding affinity of Cx43 to Gap26 was -7.0 (kcal/mol) as shown in Table 1. Gap26 binds to the pocket composed of Cx43 through hydrogen bonding, thereby interacting with Cx43 as shown in Figure 7.

Table 1: MOE score of Cx43 protein and Gap26 (kcal/mol)

Mode	Affinity (kcal/mol)	Dist from Rmsdl.b.	Best mode Rmsdu.b.
1	-7.0	0	0
2	-6.8	26.733	31.506
3	-6.8	22.801	27.665
4	-6.6	3.199	9.131
5	-6.5	23.357	27.411
6	-6.5	2.252	6.728
7	-6.5	3.295	7.345
8	-6.5	3.448	9.569
9	-6.4	3.984	9.259

Note: The binding affinity of Cx43 to Gap26 is in kcal/mol. Rmsd: A cross-sectional comparison of a group of structurally similar or related proteins to obtain differences in structural stability under these conditions. Rmsdl.b. (Rmsd upper bound) and Rmsdu.b. (Rmsd lower bound) represent the upper and lower limits of distance or angle, respectively.

4. Discussion

Studies have shown that P2X4 receptors play an important role in the pathogenesis of neuropathic pain. For example, Tsuda et al. found that neuropathic pain established after peripheral nerve injury can be reversed by P2X4 receptor blockers (22)Intrathecal delivery of P2X4 receptors activates microglia and induces allodynia in normal rats (22, 23), suggesting that excess P2X4 receptors are sufficient to cause pain. Studies have shown that astrocyte Cx43 hemichannels are thought to release cytokines after CCI to enhance synaptic transmission in the spinal cord and mediate the neuropathic pain (24); In addition, knockdown of Cx43 by RNAi can significantly alleviate pain in CCI rats, but the specific mechanism is unclear (25). Sensory disturbances and persistent pain are common side effects of peripheral neuropathy, activation of spinal cord astrocytes and expression of connexin between astrocytes significantly increased in oxaliplatin-induced peripheral neuropathy rats, however, its specific mechanism needs to be further studied (26). Cx43 is the main way to release ATP, and a large amount of ATP can cause cells to secrete a series of cytokines to activate glial cells and aggravate neuronal damage(27); P2X4 receptors are ATP-gated cation channels with high permeability to Ca^{2+} (28, 29). Therefore, Cx43 may play an important role in P2X4 receptor-mediated neuropathic pain. Gap26 is a Cx43 mimetic peptide that corresponds to amino acid residues 63-75 of Cx43 and is also a gap junction blocker (30). It was shown that Gap26 can degrade overexpressed Cx43 through the ubiquitin-proteasome pathway(31); Application of Gap26 inhibits the action of Cx43 hemichannels and gap junctions, such as blocking ATP, Ca^{2+} through connexin hemichannels (30). In the study, we found by molecular docking technique that Gap26 does have a strong affinity with Cx43 as shown in Figure7, consistent with the above findings, Gap26 would affect the opening of Cx43 hemichannels and the release of small molecules by binding to Cx43 and the function of the gap junctions formed by hemichannel docking. Western blot and immunofluorescence showed a significant increase of Cx43 expression in CCI rats, and intrathecal injection of Gap26 significantly reduced Cx43 expression and sensitivity of mechanical and thermal pain in CCI rats. In addition to the above studies, we found that Gap26 also decreased the level of P2X4 mRNA in the DRG of CCI rats. The above findings suggest that blocking CX43 relieves P2X4 receptor-mediated neuropathic pain in CCI rats.

In developing brains, glial cells have many important roles in the nervous system, neurons often form far from where they eventually settle. Thus, development involves the migration of large numbers of neurons, a process in which glial cells play a major role (32). Glial cells are the supporting cells of neurons, and neurons depend on signals released by glial cells (33). Synapses are very critical functional units in the nervous system, and there are many synapses between neurons and other cells. Synapse formation, efficiency, and maintenance are closely linked to glial signaling (34). Myelin is formed by oligo glia of the central nervous system and myelinated Schwann cells of the peripheral nervous system (35).Glial cells have many neurotransmitter receptors that are activated during synaptic activity, regulating synaptic transmission and neuronal excitability. Glial cells have molecular pumping mechanisms and intracellular enzymes that enable them to participate in the process of removing major neurotransmitters, thereby helping to terminate postsynaptic effects following transmitter secretion (36). Satellite glial cells control

the microenvironment of neurons and influence synaptic transmission(37); they also receive signals from other cells. In addition, satellite glial cells release a large number of signaling molecules to affect neighboring satellite glial cells and neurons(38, 39).

Cytokines released by glial cells have been shown to play an important role in neuropathic pain (40). Hemichannels and gap junctions composed of Cx43 are one of the main pathways in which glial cells are involved in intercellular signal communication(37, 41, 42). Knockdown of Cx43 in a spinal cord injury-induced neuropathic pain model reduces inflammation and improves functional recovery from neuropathic pain (43).Our experimental results show that blocking of Cx43 decreases the levels of cytokines such as ATP, TNF-α and IL-1β, reduces the number of activated satellite glial cells and neurons, and prevents the development of cascade amplification effects of pain mediators, effectively reducing the development of neuropathic pain. We found that in CCI rats, as shown in the results of Figure 6 TNF-α and IL-1β levels increase, and in combination with TNFR and IL-1R on satellite glial cells, a large number of satellite glial cells are activated by inflammatory factors, which in turn release more inflammatory factors (ATP, TNF-α, IL-1β), and in combination with the corresponding receptors on neurons, neuronal cells are activated, and activated neurons likewise release large amounts of inflammatory factors, creating a cascade amplification effect of inflammation. Satellite glial cells release a variety of inflammatory mediators such as ATP, TNF-α, and IL-1β; Receptors and transport proteins on the cell membrane such as P2X4R, TNFR, IL-1R can be activated; MAPKs and NF-κB are activated and further induce pain-related downstream signaling; Activated satellite glial cell Cx43 hemichannels open and release large amounts of ATP.

Mitogen-activated protein kinase (MAPK) is an important molecule that transmits signals from the cell surface to the interior of the nucleus, and activation of the MAPK cascade is central to a variety of signaling pathways(44). MAPK is quiescent in unstimulated cells; however, when cells are stimulated by cytokines, MAPK is gradually phosphorylated(45). In this study, we detected increased levels of phosphorylated p38 and ERK in CCI rats. Thus, the p38 and ERK signaling pathways are involved in the release of inflammatory factors from satellite glial cells. However, the western blot results also showed that Gap26 significantly reduced the phosphorylation levels of p38 and ERK; therefore, the reversal of neuropathic pain in CCI rats by Gap26 was associated with reduced activation of the p38 and ERK signaling pathways. In addition to the studies described above, we also found that Gap26 simultaneously reduced the levels of the P2X4 mRNA in the DRG of CCI rats. NF-κB, a protein complex that controls gene transcription and cytokine production, is involved in cellular responses to stimuli(46). The inactivated NF-κB dimer is sequestered in the cytoplasm by the repressor proteins of the IκB family, but due to its proinflammatory function, activated NF-κB can trigger neuronal dysfunction and death(47).NF-κB activation is mainly attributed to the phosphorylation of the IκB protein, which allows NF-κB to enter the nucleus(48).Study suggests chronic inflammation may involve interaction between MAPK and NF-κB signaling pathways (49). In addition, activated MAPK signaling pathway activates NF-κB and mediates the occurrence and development of inflammatory responses (50). NF-κB is a ubiquitous transcription factor that plays a key role in the expression of various inflammatory factors or proteins (46). The MAPK signaling pathway mediates the expression of various inflammatory factors, and the activation of NF-κB

is closely related to the increase in the release of inflammatory factors (51).The results of western blotting and immunofluorescence experiments confirmed that NF-κB phosphorylation levels were significantly increased in CCI rats and that large amounts of NF-κB entered the nucleus. In contrast, the Gap26 group showed significantly lower levels of phosphorylated NF-κB, and only a small amount of NF-κB was present in the nucleus. Thus, the NF-κB signaling pathway is involved in the process by which Gap26 reduces the expression of the P2X4 receptor.

In the study, we showed that ATP is an important molecule mediating the association between Cx43 and P2X4 in neuropathic pain and found that cytokines(TNF-α, IL-1β) released early mediate the onset and development of neuropathic pain. First, after peripheral nerve injury in CCI rats, inflammatory factors such as TNF-α and IL-1β are released and activate the corresponding receptors on DRG satellite glial cells by activating the p38, ERK and NF-κB signaling pathways and increasing the expression of Cx43 and P2X4 receptors on satellite glial cells. Second, the activation of glial cells is increased substantially, and large amounts of ATP are released extracellularly via the Cx43 hemichannel. Large amounts of ATP bind to P2X4 receptors on self- and adjacent satellite glial cells, and further activation of satellite glial cells occurs. Furthermore, these changes ultimately lead to a cascading amplification effect of the pain mediator. The production of pain mediators persistently excites neurons, leading to the development and persistence of neuropathic pain. However, Gap26 reduced the expression of Cx43, resulting in a decrease in the release of ATP and a decrease in the number of activated satellite glial cells and neurons, preventing the cascade amplification effect of pain mediators and effectively reducing the development of neuropathic pain.

5. Conclusion

Intrathecal injection of Gap26 can alleviate neuropathic pain and reduce P2X4 receptor expression in CCI rats, indicating that CX43 is involved in P2X4 receptor-mediated neuropathic pain in CCI rats; inflammatory factors and p38, ERK1/2MAPK and NF-κB signaling pathways may be involved in the pathophysiological process that blocking CX43 alleviates P2X4 receptor-mediated neuropathic pain in CCI rats（Figure8).

Declarations

Ethics approval and consent to participate

The Animal Management Committee of Nanchang University approved the animal experiments included in this study.

Consent for publication

Not applicable

Availability of data and materials

Data sharing is not applicable to this article as no datasets were generated or analyzed during the current study.

Competing interests

The authors declare that they have no competing interests" in this section.

Funding

This work was supported by National Natural Science Foundation of China (grant nos. 81660199 and 81260187) and Natural Science Foundation of Jiangxi Province the grant (No. 20202BAB206027)

Authors' contributions

CX: study design and final approval of manuscript. JX: study analysis, conducted the study, performed the statistical analysis, wrote the manuscript. HW, LC, HW, HH and JH: collection and assembly of data. All authors have read and approved the final version of the manuscript.

Acknowledgements

Not applicable

References

1. Baron R, Binder A, Wasner G. Neuropathic pain: diagnosis, pathophysiological mechanisms, and treatment. The Lancet Neurology. 2010;9(8):807-19.
2. Jensen TS, Finnerup NB. Allodynia and hyperalgesia in neuropathic pain: clinical manifestations and mechanisms. The Lancet Neurology. 2014;13(9):924-35.
3. Kuner R, Flor H. Structural plasticity and reorganisation in chronic pain. Nature reviews Neuroscience. 2016;18(1):20-30.
4. Meacham K, Shepherd A, Mohapatra DP, Haroutounian S. Neuropathic Pain: Central vs. Peripheral Mechanisms. Curr Pain Headache Rep. 2017;21(6):28.
5. White FA, Jung H, Miller RJ. Chemokines and the pathophysiology of neuropathic pain. Proceedings of the National Academy of Sciences of the United States of America. 2007;104(51):20151-8.
6. Yin Y, Hong J, Phạm TL, Shin J, Gwon DH, Kwon HH, et al. Evans Blue Reduces Neuropathic Pain Behavior by Inhibiting Spinal ATP Release. International journal of molecular sciences. 2019;20(18).

7. Braga AV, Costa SOAM, Rodrigues FF, Melo ISF, Morais MI, Coelho MM, et al. Thiamine, riboflavin, and nicotinamide inhibit paclitaxel-induced allodynia by reducing TNF-α and CXCL-1 in dorsal root ganglia and thalamus and activating ATP-sensitive potassium channels. Inflammopharmacology. 2020;28(1):201-13.
8. Chen G, Park C-K, Xie R-G, Berta T, Nedergaard M, Ji R-R. Connexin-43 induces chemokine release from spinal cord astrocytes to maintain late-phase neuropathic pain in mice. Brain : a journal of neurology. 2014;137(Pt 8):2193-209.
9. Xiang H-C, Lin L-X, Hu X-F, Zhu H, Li H-P, Zhang R-Y, et al. AMPK activation attenuates inflammatory pain through inhibiting NF-κB activation and IL-1β expression. Journal of neuroinflammation. 2019;16(1):34.
10. Ji RR, Xu ZZ, Gao YJ. Emerging targets in neuroinflammation-driven chronic pain. Nat Rev Drug Discov. 2014;13(7):533-48.
11. Suurväli J, Boudinot P, Kanellopoulos J, Rüütel Boudinot S. P2X4: A fast and sensitive purinergic receptor. Biomed J. 2017;40(5):245-56.
12. Stokes L, Layhadi JA, Bibic L, Dhuna K, Fountain SJ. P2X4 Receptor Function in the Nervous System and Current Breakthroughs in Pharmacology. Frontiers in pharmacology. 2017;8:291.
13. Sommer C, Leinders M, Üçeyler N. Inflammation in the pathophysiology of neuropathic pain. Pain. 2018;159(3):595-602.
14. Fields RD, Burnstock G. Purinergic signalling in neuron-glia interactions. Nature reviews Neuroscience. 2006;7(6):423-36.
15. Cekic C, Linden J. Purinergic regulation of the immune system. Nat Rev Immunol. 2016;16(3):177-92.
16. Alles SRA, Smith PA. Etiology and Pharmacology of Neuropathic Pain. Pharmacol Rev. 2018;70(2):315-47.
17. García-Vega L, O'Shaughnessy EM, Jan A, Bartholomew C, Martin PE. Connexin 26 and 43 play a role in regulating proinflammatory events in the epidermis. J Cell Physiol. 2019.
18. Nielsen MS, Axelsen LN, Sorgen PL, Verma V, Delmar M, Holstein-Rathlou NH. Gap junctions. Compr Physiol. 2012;2(3):1981-2035.
19. Beyer EC, Berthoud VM. Gap junction gene and protein families: Connexins, innexins, and pannexins. Biochim Biophys Acta Biomembr. 2018;1860(1):5-8.
20. Nielsen MS, Axelsen LN, Sorgen PL, Verma V, Delmar M, Holstein-Rathlou N-H. Gap junctions. Comprehensive Physiology. 2012;2(3):1981-2035.
21. Bennett GJ, Xie YK. A peripheral mononeuropathy in rat that produces disorders of pain sensation like those seen in man. Pain. 1988;33(1):87-107.
22. Tsuda M, Shigemoto-Mogami Y, Koizumi S, Mizokoshi A, Kohsaka S, Salter MW, et al. P2X4 receptors induced in spinal microglia gate tactile allodynia after nerve injury. Nature. 2003;424(6950):778-83.
23. Tsuda M, Inoue K, Salter MW. Neuropathic pain and spinal microglia: a big problem from molecules in "small" glia. Trends Neurosci. 2005;28(2):101-7.

24. Chen G, Park CK, Xie RG, Berta T, Nedergaard M, Ji RR. Connexin-43 induces chemokine release from spinal cord astrocytes to maintain late-phase neuropathic pain in mice. Brain. 2014;137(Pt 8):2193-209.
25. Ohara PT, Vit JP, Bhargava A, Jasmin L. Evidence for a role of connexin 43 in trigeminal pain using RNA interference in vivo. J Neurophysiol. 2008;100(6):3064-73.
26. Tonkin RS, Bowles C, Perera CJ, Keating BA, Makker PGS, Duffy SS, et al. Attenuation of mechanical pain hypersensitivity by treatment with Peptide5, a connexin-43 mimetic peptide, involves inhibition of NLRP3 inflammasome in nerve-injured mice. Exp Neurol. 2018;300:1-12.
27. Huang TY, Cherkas PS, Rosenthal DW, Hanani M. Dye coupling among satellite glial cells in mammalian dorsal root ganglia. Brain Res. 2005;1036(1-2):42-9.
28. Zhang WJ, Zhu ZM, Liu ZX. The role of P2X4 receptor in neuropathic pain and its pharmacological properties. Pharmacol Res. 2020;158:104875.
29. Tsuda M. [Mechanisms underlying the pathogenesis of neuropathic pain revealing by the role of glial cells]. Nihon Shinkei Seishin Yakurigaku Zasshi. 2015;35(1):1-4.
30. Desplantez T, Verma V, Leybaert L, Evans WH, Weingart R. Gap26, a connexin mimetic peptide, inhibits currents carried by connexin43 hemichannels and gap junction channels. Pharmacol Res. 2012;65(5):546-52.
31. Li X, Zhao H, Tan X, Kostrzewa RM, Du G, Chen Y, et al. Inhibition of connexin43 improves functional recovery after ischemic brain injury in neonatal rats. Glia. 2015;63(9):1553-67.
32. Rakic P. Elusive radial glial cells: historical and evolutionary perspective. Glia. 2003;43(1):19-32.
33. Jessen KR, Mirsky R. Signals that determine Schwann cell identity. J Anat. 2002;200(4):367-76.
34. Barres BA, Smith SJ. Neurobiology. Cholesterol--making or breaking the synapse. Science (New York, NY). 2001;294(5545):1296-7.
35. Jessen KR. Glial cells. Int J Biochem Cell Biol. 2004;36(10):1861-7.
36. Walz W. Role of astrocytes in the clearance of excess extracellular potassium. Neurochem Int. 2000;36(4-5):291-300.
37. Haydon PG, Carmignoto G. Astrocyte control of synaptic transmission and neurovascular coupling. Physiol Rev. 2006;86(3):1009-31.
38. Montana V, Malarkey EB, Verderio C, Matteoli M, Parpura V. Vesicular transmitter release from astrocytes. Glia. 2006;54(7):700-15.
39. Hanani M. Satellite glial cells in sensory ganglia: from form to function. Brain Res Brain Res Rev. 2005;48(3):457-76.
40. Scholz J, Woolf CJ. The neuropathic pain triad: neurons, immune cells and glia. Nat Neurosci. 2007;10(11):1361-8.
41. Komiya H, Shimizu K, Ishii K, Kudo H, Okamura T, Kanno K, et al. Connexin 43 expression in satellite glial cells contributes to ectopic tooth-pulp pain. J Oral Sci. 2018;60(4):493-9.

42. Theis M, Söhl G, Eiberger J, Willecke K. Emerging complexities in identity and function of glial connexins. Trends Neurosci. 2005;28(4):188-95.
43. Chen MJ, Kress B, Han X, Moll K, Peng W, Ji RR, et al. Astrocytic CX43 hemichannels and gap junctions play a crucial role in development of chronic neuropathic pain following spinal cord injury. Glia. 2012;60(11):1660-70.
44. Inoue T, Boyle DL, Corr M, Hammaker D, Davis RJ, Flavell RA, et al. Mitogen-activated protein kinase kinase 3 is a pivotal pathway regulating p38 activation in inflammatory arthritis. Proc Natl Acad Sci U S A. 2006;103(14):5484-9.
45. Fang JY, Richardson BC. The MAPK signalling pathways and colorectal cancer. Lancet Oncol. 2005;6(5):322-7.
46. Sehnert B, Burkhardt H, Dübel S, Voll RE. Cell-Type Targeted NF-kappaB Inhibition for the Treatment of Inflammatory Diseases. Cells. 2020;9(7).
47. Ghosh S, Hayden MS. New regulators of NF-kappaB in inflammation. Nat Rev Immunol. 2008;8(11):837-48.
48. Perkins ND. Integrating cell-signalling pathways with NF-kappaB and IKK function. Nat Rev Mol Cell Biol. 2007;8(1):49-62.
49. Ramalingam P, Poulos MG, Lazzari E, Gutkin MC, Lopez D, Kloss CC, et al. Chronic activation of endothelial MAPK disrupts hematopoiesis via NFKB dependent inflammatory stress reversible by SCGF. Nat Commun. 2020;11(1):666.
50. Ke J, Cai G. Effect of IL-33 on pyroptosis of macrophages in mice with sepsis via NF-κB/p38 MAPK signaling pathway. Acta Cir Bras. 2021;36(5):e360501.
51. El-Agamy DS, El-Harbi KM, Khoshhal S, Ahmed N, Elkablawy MA, Shaaban AA, et al. Pristimerin protects against doxorubicin-induced cardiotoxicity and fibrosis through modulation of Nrf2 and MAPK/NF-kB signaling pathways. Cancer Manag Res. 2019;11:47-61.
52. Gu Y, Chen Y, Zhang X, Li GW, Wang C, Huang LY. Neuronal soma-satellite glial cell interactions in sensory ganglia and the participation of purinergic receptors. Neuron Glia Biol. 2010;6(1):53-62.

Figures

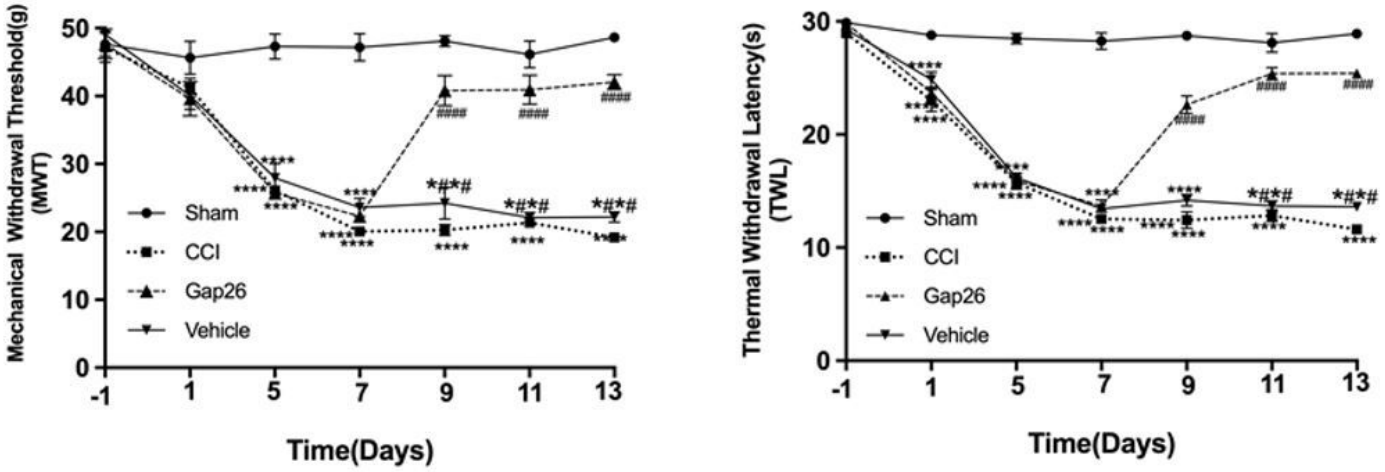

Figure 1

Gap26 reduces mechanical and thermal pain sensitivity in CCI rats. Panel A show that an intrathecal injection of Gap26 on postoperative Day 7 significantly reduced abnormal mechanical pain in CCI rats. Panel B shows a significant reduction in thermal pain sensitivity in CCI rats after the intrathecal injection of Gap26 on postoperative Day 7. ****P<0.0001, compared with the sham group; ####P<0.0001, compared with the CCI group; *#*#P<0.0001, compared with the Gap26 group.

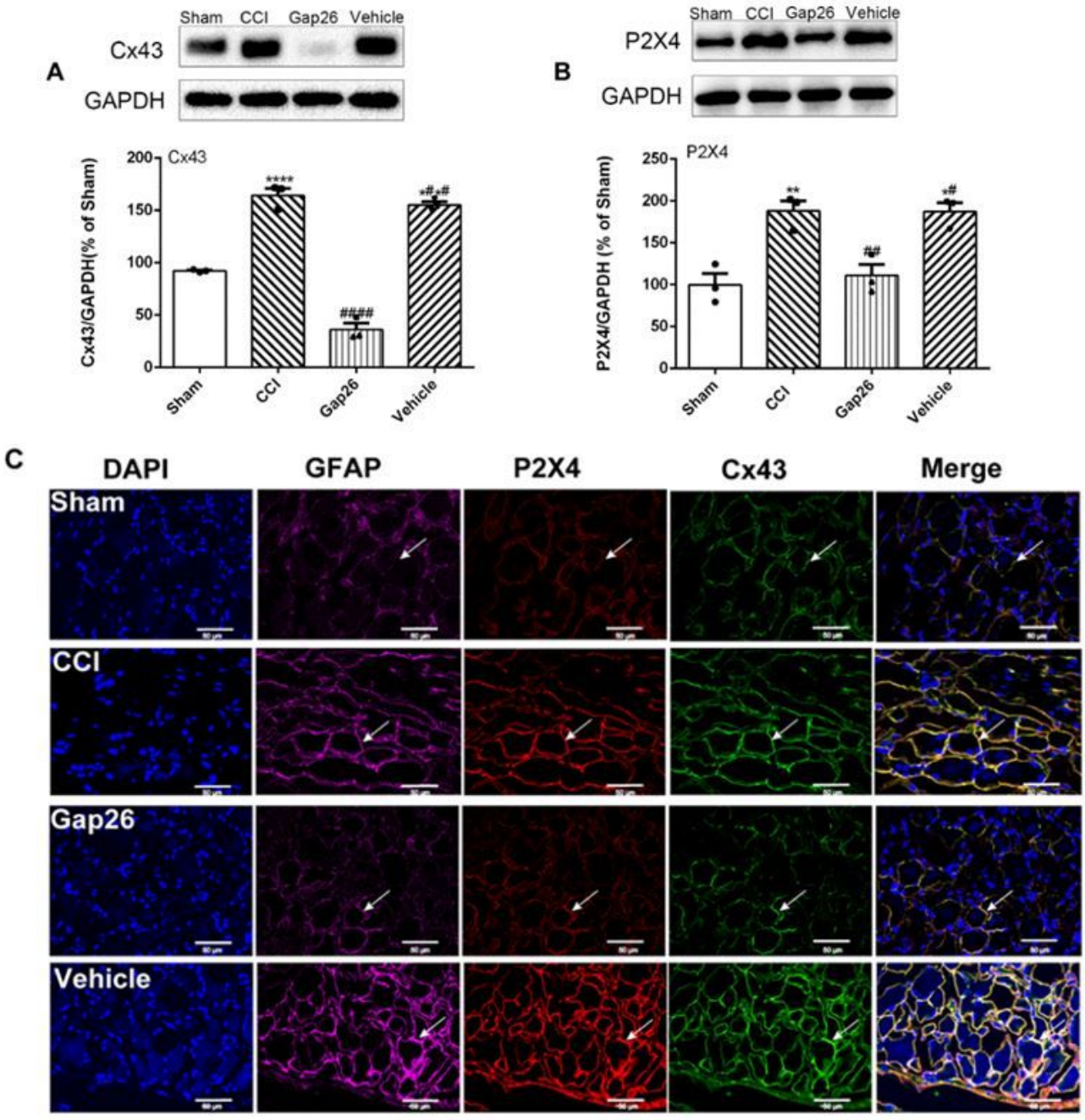

Figure 2

Effect of an intrathecal injection of Gap26 on the expression of the Cx43 and P2X4 proteins in the DRG of CCI rats. Panel A show the electrophoretic bands for Cx43andp2x4 proteins and their corresponding GAPDH bands in each group. Panel B shows the quantification of Cx43 and P2X4 levels in the DRGs of CCI rats. The western blot result is presented as the fold change relative to the sham control. Panel C, Laser scanning confocal image showing Cx43 (green) and P2X4 (red) colocalized with GFAP (magenta) (40x). **P<0.01, ****P<0.0001 compared with the sham group; ##P<0.01, ####P<0.0001 compared with the CCI group; *#P<0.01, *#*#P<0.0001 compared with the Gap26 group.

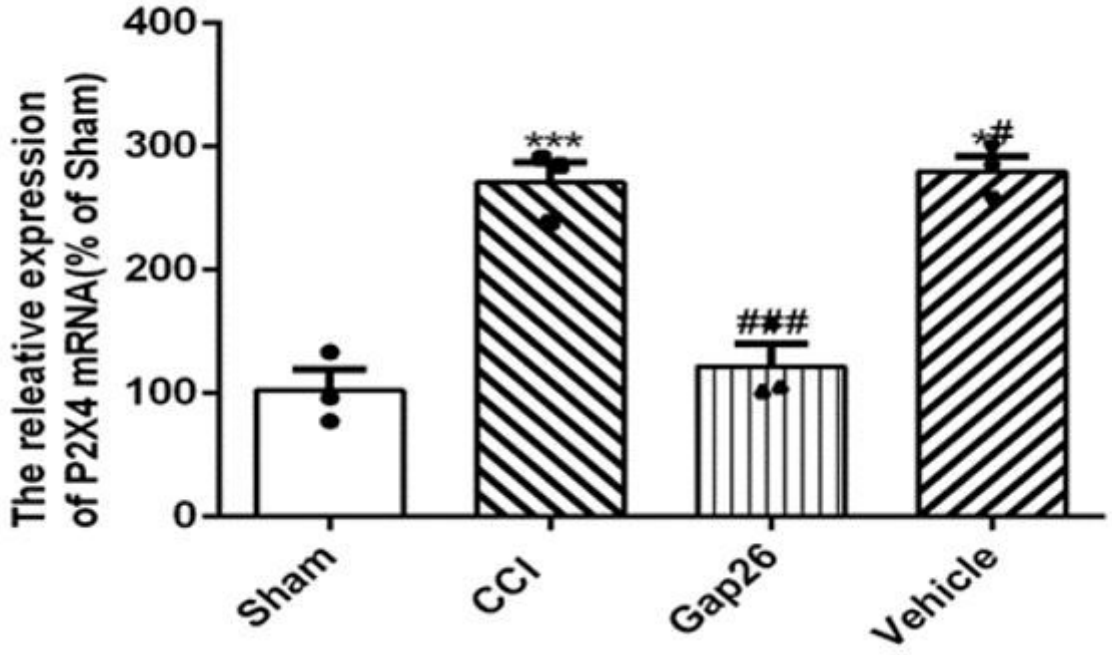

Figure 3

Effect of Gap26 on the level of P2X4 mRNA in the DRGs of CCI rats. Gap26 reduced P2X4 mRNA levels in the DRG of CCI rats. **P<0.01, compared with the sham group; $^{\#\#}$P<0.01, compared with the CCI group; $^{*\#}$P<0.01, compared with the Gap26 group.

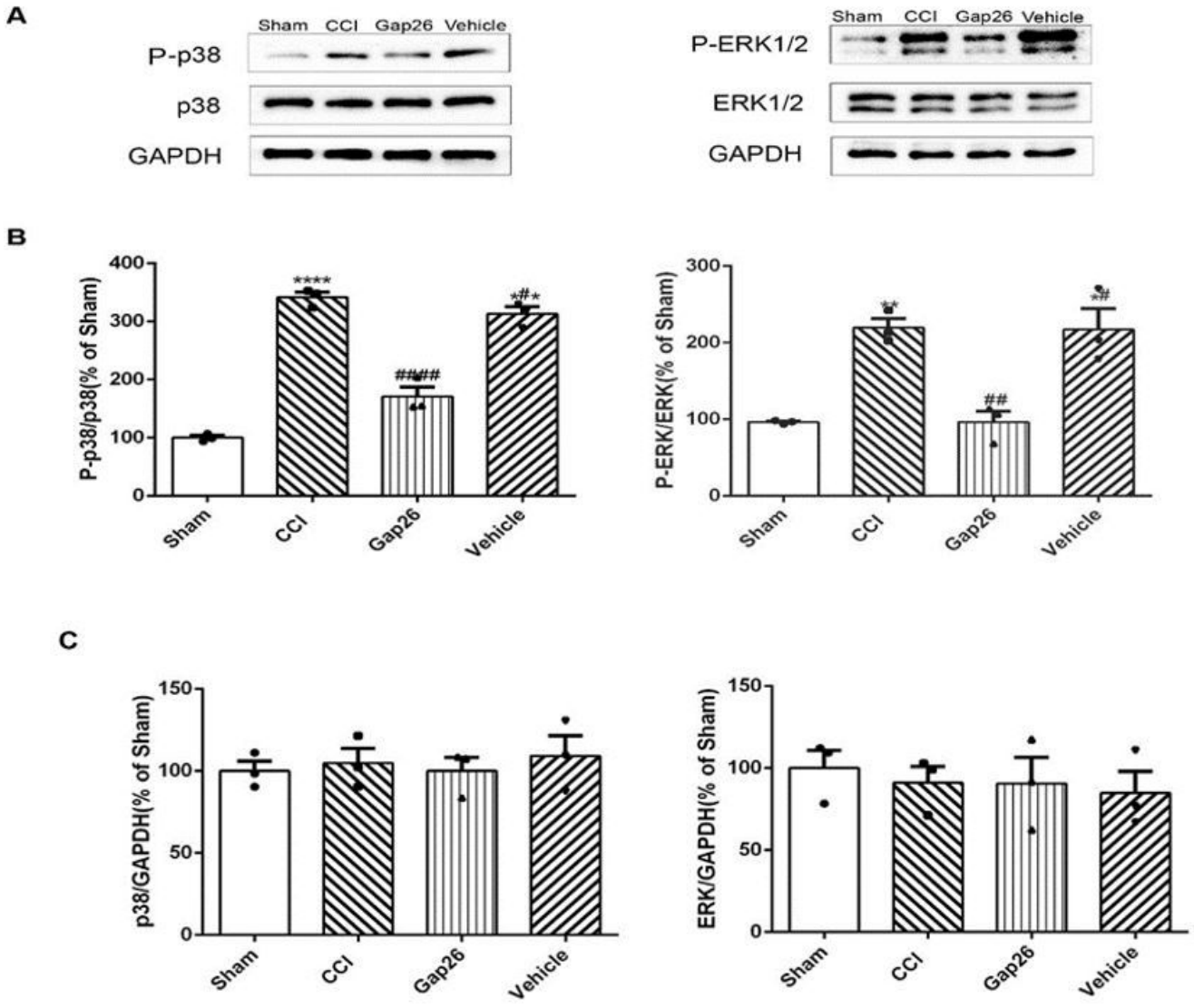

Figure 4

Levels of the phosphorylated p38 and ERK proteins in the DRG of CCI rats. Panel A show the electrophoretic bands for the P-p38,P-ERKproteins and their corresponding GAPDH bands. Panels B show the quantification of p38 and ERK phosphorylation in the DRG of CCI rats. The western blot result is presented as the fold change relative to the sham control. Panels C show the quantification of p38and ERK in DRG of CCI rats. The western blot result is presented as the fold change relative to the sham control. **P<0.01, ****P<0.0001, compared with the sham group; $^{\#\#}$P<0.01, $^{\#\#\#\#}$P<0.0001 compared with the CCI group; $^{*\#}$P<0.01, $^{*\#*}$P<0.001 compared with the Gap26 group.

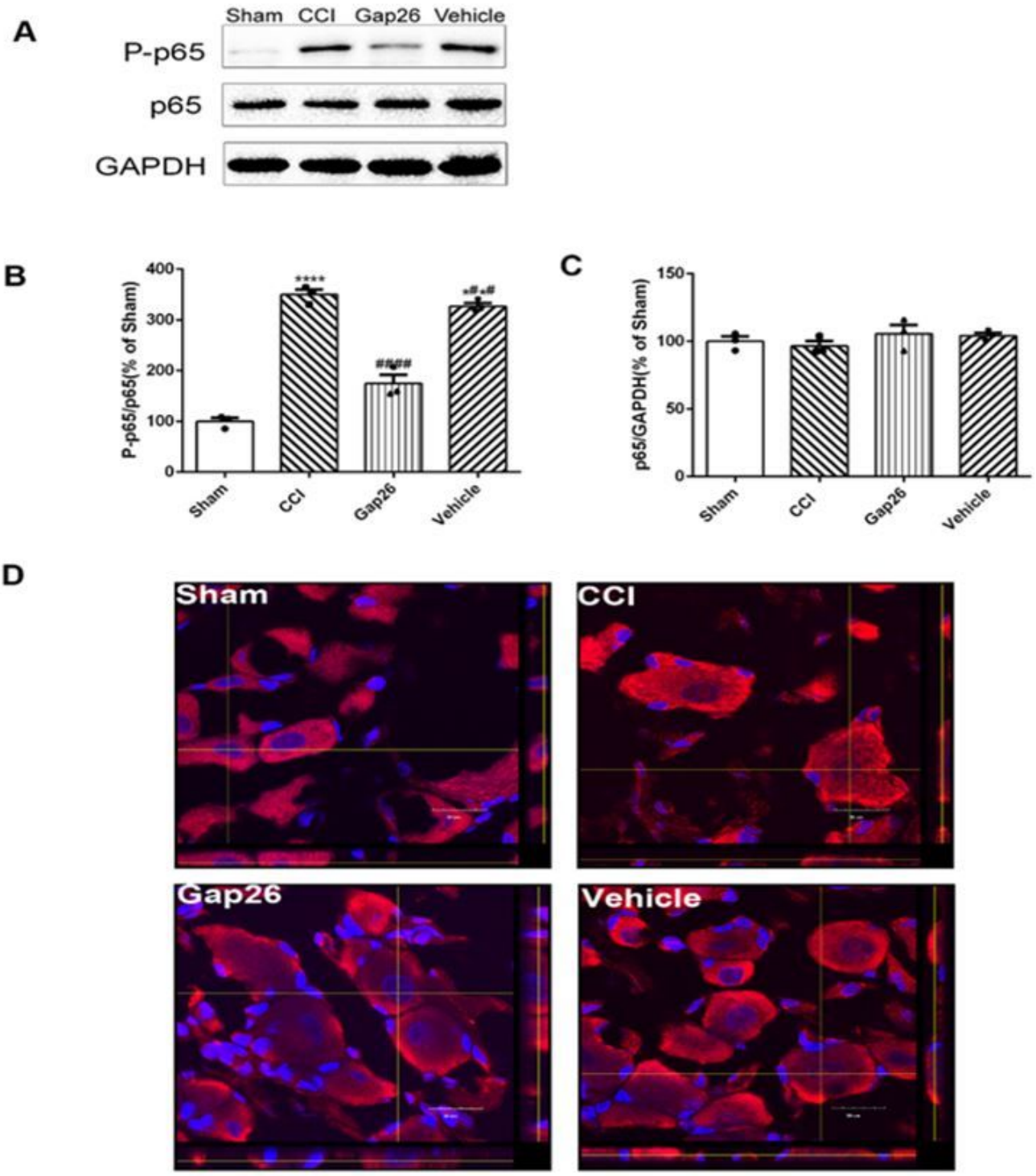

Figure 5

Levels of the phosphorylated NF-κB protein in the DRGs of CCI rats. Panel A show the electrophoretic bands for the P-p65 and p65 proteins and their corresponding GAPDH bands. Panels B and C show the quantification of p65 phosphorylation in the DRG of CCI rats. The western blot result is presented as the fold change relative to the sham control. Panel D shows laser scanning confocal microscopy images of the nuclear localization of p65 in each group. ****P<0.0001, compared with the sham group; ####P<0.0001 compared with the CCI group; *#*#P<0.0001 compared with the Gap26 group.

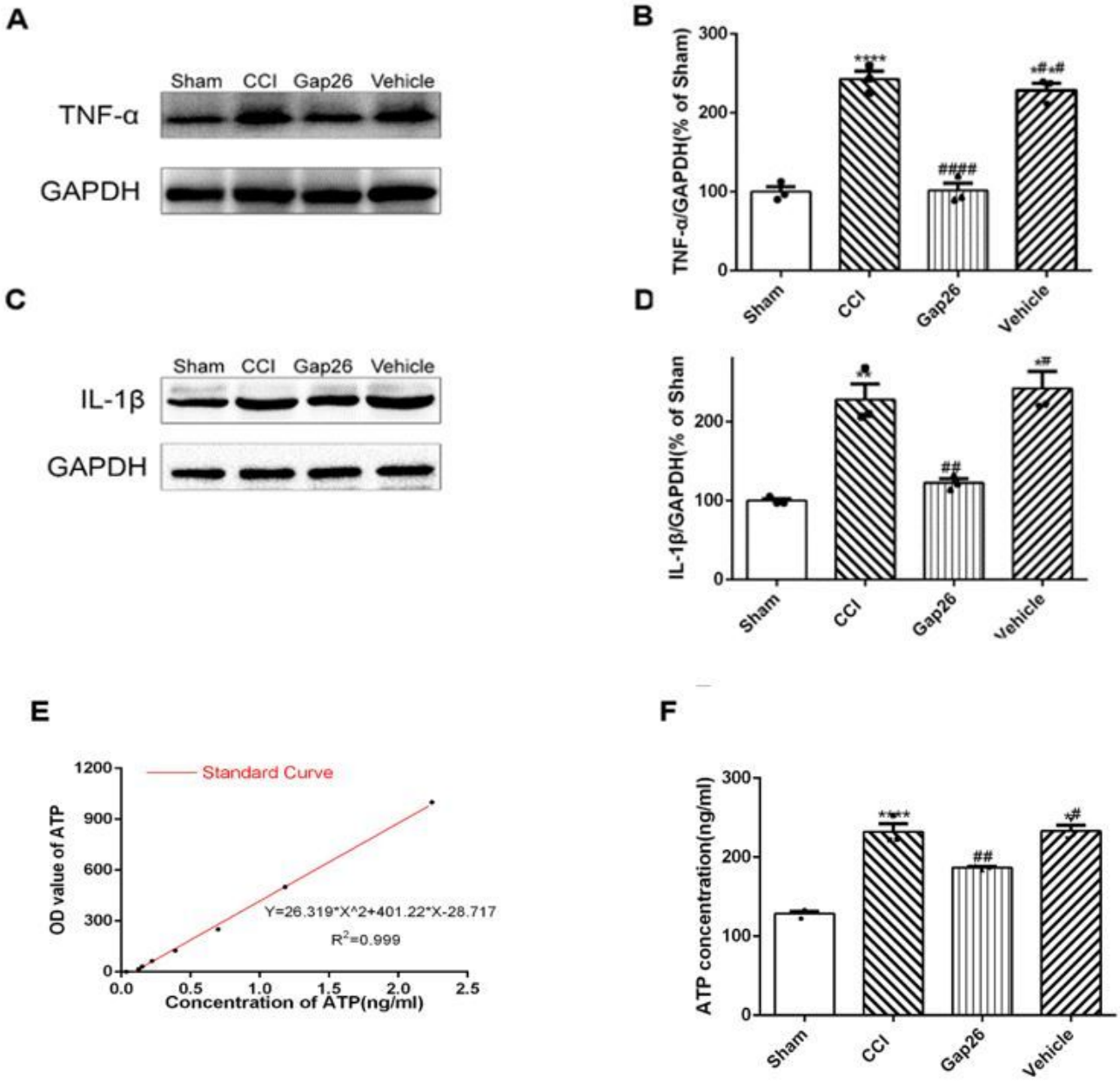

Figure 6

Gap26 reduced the expression of TNF-α, IL-1β, ATP in CCI rats. Panel A and C show the electrophoretic bands for TNF-α and IL-1β proteins and their corresponding GAPDH bands in each group. Panel B and D shows the quantification of TNF-α and IL-1β levels in the DRGs of CCI rats. The western blot result is presented as the fold change relative to the sham control. Panel E shows the standard curve of the ELISA: the relationship between the rat serum ATP concentration and the OD at 450 nm. Panel F shows the quantification of ATP levels in CCI rats. The ELISA result is presented as the fold change relative to the sham control. The ELISA result is presented as the fold change relative to the sham control. ****P<0.0001,

compared with the sham group; ##P<0.01, ####P<0.0001, compared with the CCI group; *#P<0.01, compared with the Gap26 group.

Figure 7

The results of molecular docking. Panel A and B showed the positive and top view. Panel C showed the binding pocket of Cx43 and Gap26. Panel D showed the best binding site of Cx43 and Gap26, the yellow dotted line was the hydrogen bond.

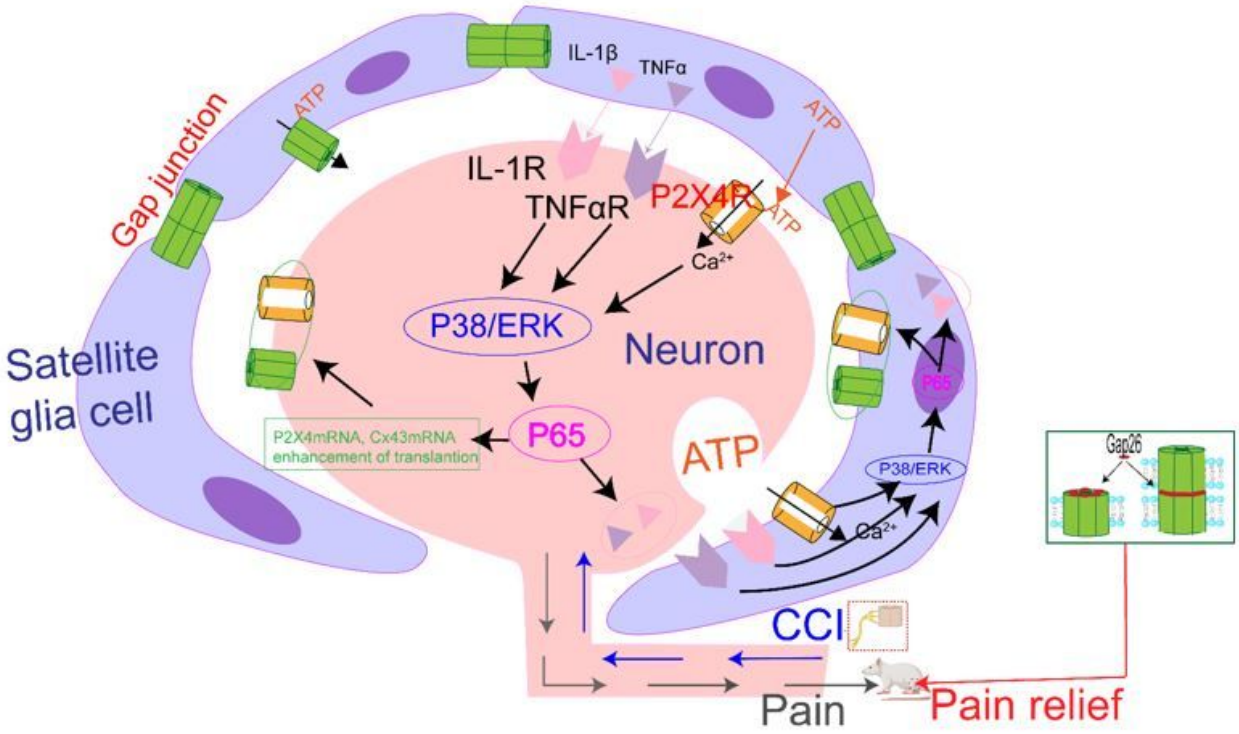

Figure 8

Blockade of Cx43 alleviates neuropathic pain in CCI rats and its possible mechanism. Primary afferents, glia, and leukocytes release early inflammatory factors such as TNF-α and IL-1β, which bind to TNFR and IL-1R on satellite glia, respectively, induce DRG satellite glia activation and increase Cx43 and P2X4 expression. Numerous cytokines are released extracellularly through Cx43 hemichannels. ATP activates more satellite glial cells through a cascade effect, ultimately leading to the production of pain mediators that continuously excite neurons. This figure is referenced from Yanping Gu et al(52).